PROCEEDINGS OF THE INTERNATIONAL CONFERENCE NANOMATERIALS: APPLICATIONS AND PROPERTIES
Vol. **2** No 2, 02PCN28(4pp) (2013)

Surfactant Assisted Synthesis of $LiFePO_4$ Nanostructures via Hydrothermal Processing

S. C. °Zhang*, G. R. °Liu†, X. °Wei, X. X. °Lu

School of Materials Science &Engineering, Beijing University of Aeronautics & Astronautics, Beijing 100191, China

(Received 09 June; published online 02 September 2013)

$LiFePO_4$ is a potential cathode candidate for of secondary lithium batteries due to its low-cost, outstanding thermal stability and innocuity. In this paper, pure $LiFePO_4$ obtained by hydrothermal method using cetyltrimethyl ammonium bromide (CTAB) as surfactant. $LiFePO_4$ particles produced without any surfactant showed typical morphologies of perfect octahedral with size of ~1μm. For products prepared with addition CTAB, the amount of surfactant controlled the growth of $LiFePO_4$ crystals, with which different morphologies of plate, grains and flower-like structures were produced. Plate products displayed a capacity of 145.70 mAh•g^{-1} at 0.1*C*, which was superior to others. The results indicated the electrochemical performance depends crucially on the size and structure of active materials.

Keywords: $LiFePO_4$, Hydrothermal Method, Surfactant Assistance, Cathode , Nanoparticles.

PACS numbers: 81.07.Bc, 81.16.Dn, 82.45.Yz

1. INTRODUCTION

Lithium-ion batteries (LIBs) have been developed and applied successfully in the portable electronic devices, due to their low cost, safety and long operational life. Now the large-scale LIBs are growing in popularity for use in electric vehicles (EV) and hybrid electric vehicles (HEVs). Commercial LIBs utilize mainly cobalt-based oxides as the cathode.[1] However, metastable $LiCoO_2$ can easily lose oxygen while overcharging, which increases the probability of overheating and electrolyte decomposition, and its high cost and toxicity prevent it from large-scale or biomedical applications. Since pioneering work proposed by Padhi et al. in 1997,[2, 3] olivine $LiFePO_4$ has been intensively investigated as one of alternative cathode materials, owing to its low cost, outstanding thermal stability and abundance of raw materials.[4] Olivine-type $LiFePO_4$ has an orthorhombic cell, which accommodates four units of $LiFePO_4$. In one unit, all four oxygen ions build strong covalent bonds with P^{5+} to form the PO_4^{3-} tetrahedral polyanion and stabilize the entire three-dimensional framework. The steady structure provides stable performance and extreme safety during the operation. In addition, it shows good cycle stability because of its structural similarity between the charged and discharged states. [5]. Olivine-type $LiFePO_4$ has a flat voltage profile of about 3.4V vs. Li/Li^+ and a high theoretical capacity of 170mAh•g^{-1}. However, the main obstacles for achieving a perfect performance of $LiFePO_4$ at ambient temperature are its very low electronic conductivity and poor diffusion of lithium ions, which limit its commercial application such as in EVs and HEVs [6]. To overcome the drawback of low conductivity, $LiFePO_4$/electronic-conductor composites are explored by coating an electronically conductive phase [7-9]. Minimizing the particle size is an effective way to enhance the lithium-ion diffusion [10~13], because a small and homogeneous particle size distribution can shorten the diffusion distance of lithium ions.

A variety of methods have been reported to synthesis $LiFePO_4$ such as solid reaction [6, 10], sol-gel method [14], and hydrothermal process [15, 16], etc. Both of solid reaction and sol-gel methods usually contain a complicated procedure and a longtime sintering process, which result in large-size of particles and impurities at the same time. Hydrothermal synthesis has a lot of advantages such as low synthesis temperature, inexpensiveness and high productive rate, which is an alternative method to synthesize particles with small and homogeneous particle size distribution. The process of $LiFePO_4$ crystal growth under hydrothermal condition was described by S. Yang [17]. Different synthesis routes of obtaining $LiFePO_4$ were compared, showing that the product achieved by hydrothermal method exhibits an initial capacity of 120 mAh.g^{-1} and good cycle performance [11]. Herein, we report a hydrothermal approach to obtained $LiFePO_4$ with different size and morphologies by introducing surfactants.

2. EXPERIMENTAL

2.1 Preparation and characterization of $LiFePO_4$ nanostructures

$LiFePO_4$ particles were prepared by hydrothermal method using Cetyltrimethyl Ammonium Bromide (CTAB) as surfactant. The addition of surfactant was 0.2g, 0.5g and 1g, respectively. In typical procedure, 1mol/L solution was prepared from $LiOH·H_2O$, $FeSO_4·7H_2O$ and H_3PO_4 (the molar ratio of Li:Fe:P is 3:1:1): $LiOH·H_2O$ was dissolved in the solvent with continuous stirring and N_2 atmosphere. H_3PO_4, $FeSO_4·7H_2O$ and CTAB were then added into the solution. Subsequently, the solution was taken into a 40mL Teflon-lined stainless steel autoclave and the reactors were maintained at 180℃ for 4h. After cooling to the room temperature, the final solution was filtered and dried at 60 ℃ for 10h in a vacuum oven.

X-ray diffraction (XRD) patterns were recorded at room temperature using a Rigaku D/MAX 2000 PC

* csc@buaa.edu.cn
† liugr1108@gmail.com

diffractometer with Cu Kα radiation (λ = 1.5406Å) with the scanning rate of 6°/min. The morphologies of the samples were observed by a field-emission scanning electron microscopy (Apollo 300). Detailed structural properties of the obtained product were investigated by transmission electron microscopy (TEM, JEM-2100F, JEOL).

2.2 Electrochemical measurements

The electrochemical measurements of the samples were studied by simulated cells assembled in an Ar-filled glove box (MB-10-G with TP170b/mono, MBRAUN) using lithium foil as anode, 1M $LiPF_6$/EC+DMC (1:1 in volume) as electrolyte, and Celgard 2300 membrane as separator. Electrodes consisting of 75 wt% of $LiFePO_4$, 10 wt% of polyvinylidene fluoride (PVDF) and 15 wt% carbon black were played as cathode in the cells. The galvanostatic charge-discharge measurements were performed using a battery test system (NEWARE BTS-610, Neware Technology Co., Ltd., PR China) at a constant current density, with cut off voltage of 2.5-4.2V (vs. Li/Li^+).

3. RESULTS AND DISCUSSION

3.1 Structure and Morphology

We marked the blank product synthesized by hydrothermal method as A. The symbols for samples with the surfactant addition of 0.2g, 0.5g and 1g were B, C and D.

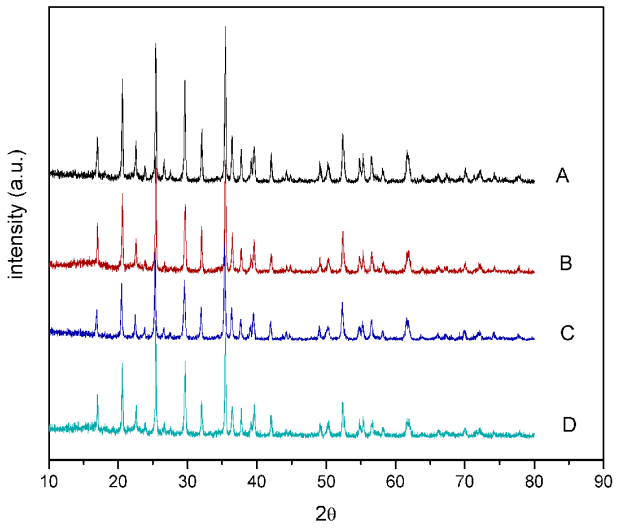

Fig. 1 – XRD patterns of the $LiFePO_4$ synthesized in different concentration of CTAB. The amount of CTAB is (A) blank sample, (B) 0.2g, (C) 0.5g, (D) 1g

Fig. 1 illustrates the X-ray diffraction patterns of the samples synthesized by hydrothermal method. All samples are identified as perfectly single-phase olivine structure indexed to orthorhombic Pnma space group, without any second phase or impurities observed, i.e. the addition of surfactant does not generate impurities or cause any phase transformation of the samples. According to Sherrer formula, the particle size of sample B, C, D is smaller than that of sample A, indicating that the size of particles is affected by the presence of surfactant.

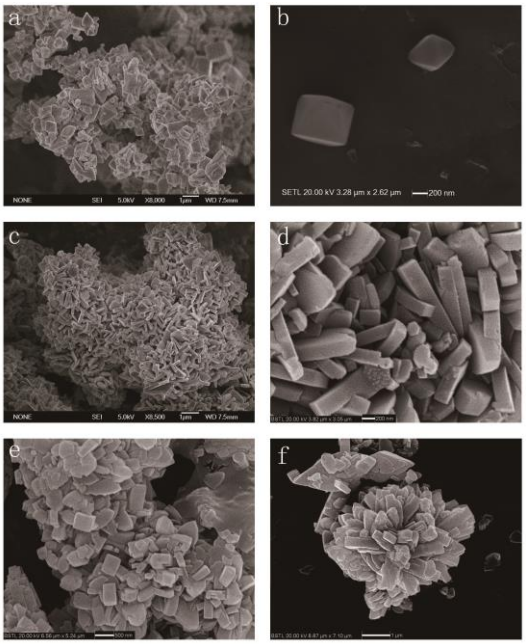

Fig. 2 – SEM images of $LiFePO_4$: (a) and (b) sample A without CTAB; (b) and (c) sample B, with addition of CTAB 0.2g; (c) sample C, CTAB 0.5g; (d) sample D, CTAB 1g.

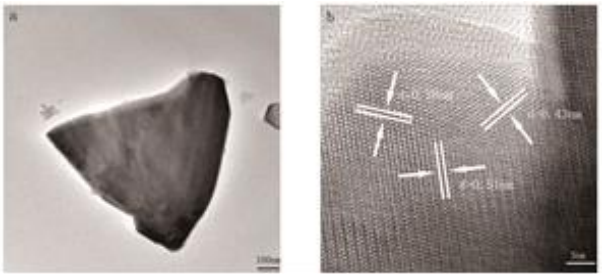

Fig. 3 TEM (a) and HRTEM (b) images of sample B.

Fig. 2 shows the morphological variation of as-prepared samples with different amount of surfactant. The size of the sample A displays variously from 500nm to 1μm. Most of the particles exhibit perfect morphology of octahedron (Fig.2a and 2b). According to literatures, the morphology of product strongly depends on reaction materials, synthesis temperature and the concentration [17-19]. The reaction condition in our study is helpful to the crystal growth in three dimensional. And then, the grains grow into octahedral crystal. It should be noted that blank sample synthesized by hydrothermal method are irregular. As is shown in Fig.2c to 2f, the product morphologies are altered by the addition of CTAB. A plate-architecture (sample B) about 200nm in width (Fig.2c and d) is obtained at the CTAB amount of 0.2g. Fig.3 shows the TEM and HRTEM images of sample B. A single plate with 1μm width shows clear lattice fringes with d-spacing of 0.28nm, 0.43nm and 0.51nm, corresponding to the (020), (011) and (031) planes of $LiFePO_4$. The size and morphologies of particles are changing with increasing concentration of addition. Fig.2e exhibits sample C with smaller grains obtained at the surfactant addition of 0.5g. When the addition of CTAB increases to 1g, a flower-like structure is achieved for sample D (Fig.2f): Each "flower" consists of a large amount of small grains, which grow from the same center to all directions.

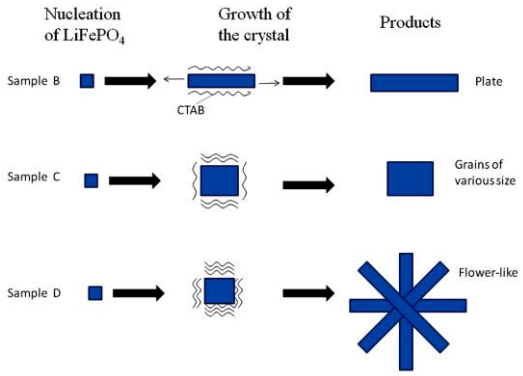

Fig. 4 – The formation process of $LiFePO_4$ with different concentration of CTAB

Surfactant plays an important role in directing the growth of such unique structure along certain growth direction [20, 21]. Fig.4 depicts the influence of surfactant during the formation process of $LiFePO_4$. CTAB is absorbed around the nucleation to suppress the growth of specific faces of crystal, while growth rate in the other faces is greater. Therefore, the product particles represent special morphology different from the sample prepared without surfactant. $LiFePO_4$ grows into the highly ordered plate architectures at the addition of CTAB with low concentration (just like sample B). When the CTAB concentration increases, the surfactant molecules trap the small grains and prevent them from growing. When the addition of CTAB is up to 1g, each crystal is trapped by CTAB micelles, and the crystal growth is suppressed temporarily. Subsequently, growth of various new directions would break the barrier of micelles, owing to the excessive supply of ions from the solution. Finally, product represents the flower-like morphology.

3.2 Electrochemical performance

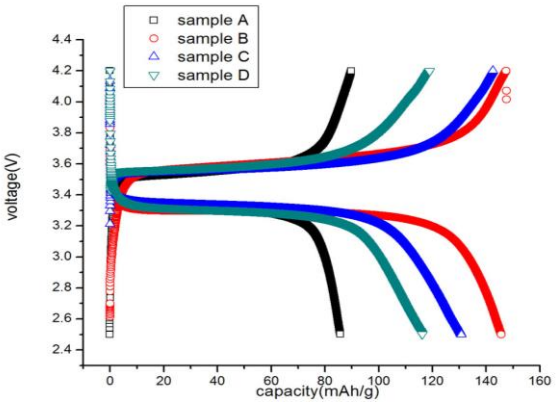

Fig. 5 – Initial charge-discharge curves of the samples

The initial charge-discharge curves of all the samples at 0.1*C* in the corresponding cells are shown in Fig. 5. Sample B delivers the highest discharge capacity of 145.70 mAh·g^{-1} at 0.1*C*, while the lowest discharge capacity of 85.78 mAh·g^{-1} is exhibited by sample A. The sample C and D display the capacity of 120.78 and 116.21 mAh·g^{-1}, respectively.

Li^+ ions diffuse along *b* direction in olivine-type $LiFePO_4$ [5], and the electrochemical performance is related to the lattice parameters of materials. The lattice parameters of the samples calculated from the experimental data of XRD patterns are listed in the Table 1. It can be seen that blank product has a lower *c*, compared to samples obtained with CTAB. The value of *a* declines with increasing concentration of CTAB. According to previous study [22], a larger value of a/c contributes to a higher specific capacity. The initial capacity of the $LiFePO_4$ obtained monotonically increases with increasing value of a/c. In the meantime, the lattice parameters are considered to be partly affected by the crystallinity of the products [23], while the presence of surfactant decreases crystallinity of the samples according to XRD results. As shown in Table 1, the value of a/c decreases with adding more CTAB. Therefore, sample B displays the highest capacity corresponding to its largest value of a/c.

Table 1 – The initial capacity of the samples towards to the lattice constants of the samples.

	a	b	c	a/c	Initial capacity
Sample A	10.3286	6.0188	4.7030	2.1962	85.78 mAh·g^{-1}
Sample B	10.3821	6.01376	4.7154	2.2018	145.70 mAh·g^{-1}
Sample C	10.3609	6.0146	4.7090	2.2002	120.78 mAh·g^{-1}
Sample D	10.3201	5.9982	4.7105	2.1909	116.21 mAh·g^{-1}

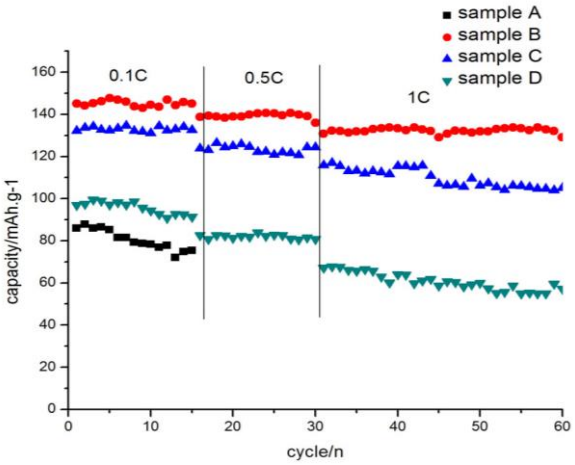

Fig. 6 – Cycle performances of the samples at different rate.

As an important performance of electrode material, it is crucial to enhance high rate capability for the commercial application of $LiFePO_4$. In this paper, products are discharged at different rate: 0.1*C*, 0.5*C* and 1*C*. Fig. 6 shows the cycle performance of all the samples over the voltage range between 2.5 V and 4.2 V. At 0.1*C*, $LiFePO_4$ of sample A presents an obvious capacity fade after 15 cycles. Sample B, C and D display good cycle performance at the low rate. The initial capacities of sample B, C and D are 138.74, 123.86 and 82.62 mAh·g^{-1}, respectively. The capacity fades of all samples is less than 1% after 15 cycles. Sample B exhibits a high capacity of 130.74 mAh·g^{-1} at the rate of 1*C*, with even no capacity fade at 30th cycle. The size and specific structure of Sample B would improve the immersion of electrolyte and reduce the distance of Li^+ diffusion from surface to center during charge/discharge. However, the specific capacities of sample C and D sharply decrease to 115.9 and 67.2mAh·g^{-1}, respectively. After 30 cycles,

sample C represents a capacity of 105.02mAh·g^{-1}, which is 90.6% of the initial capacity. And sample D shows 84.0% capacity as high as its initial discharge capacity after 30 cycles. The results of cycling tests indicate that the plate structure of sample B reduces the diffuse distance of electronics effectively; however, sample C with smaller size has a relatively low capacity, owing to its low degree of crystallinity. During the process of lithium insertion or extraction, the electronics have to diffuse from surface to center. However, in the flower-like structure of sample D, the active materials near the center of particle contribute very little to the capacity, especially at high rate charge/discharge. That is why sample C exhibits a low initial capacity and a terrible cycle performance.

4. CONCLUSION

Pure $LiFePO_4$ particles are synthesized by hydrothermal method in an aqueous solution using CTAB as surfactant. $LiFePO_4$ octahedron particles are obtained by hydrothermal method without presence of any surfactant. By adding different amount of CTAB, products show various morphologies. When the addition of CTAB is 0.2g, plate particles are obtained. With the increase of surfactant, the irregular grains and flower-like particles are produced, because of the adsorption of surfactant molecules on the crystal surface, which inhibits the growth of specific directions. Moreover, the amount of CTAB is essential for the formation of ordered architectures. The electrochemical performances are compared among the samples with different structure. The sample with plate morphology delivers a high initial capacity of 145.70 mAh·g^{-1}, which shows good cyclability at 0.1*C*. The plate-structure $LiFePO_4$ also represents excellent cycle performance with nearly no capacity fading after 30 cycles at 1*C*.

AKNOWLEDGEMENTS

This work was supported by the National Basic Research Program of China (2013CB934000), National Natural Science Foundation of China (51074011 and 51274017) and National 863 Program (2007AA03Z231 and 2011AA11A257).

REFERENCES

1. K. Mizushima, P.C. Jones, P. J. Wiseman, *Mater Res Bull*, **15**, 783 (1980).
2. A. K. Padhi, J. B. Goodenough, *Electrochem. Soc.,* **144**,1188(1997).
3. H. Xu, X. F. Guo, J. L. Sang, *Inorgan. Chem. Indust.*, **3**, 5 (2009).
4. M. Takahashi, S. Tobishima, T. Koji. *Sol. Stat. Ionics*, **148**, 283 (2002).
5. C. Y. Ouyang, S. Q. Shi, Z. X. Wang, et al.,*Phys. Rev.B,* **69**, 104303(2004).
6. Y. Q. Wang, J. L. Wang, J. Yang, N. Yanna., *Adv. Func. Mater.*, **16**, 2135 (2006).
7. C. Y. Lai, Q. J. Xu, H. H. Ge, G.D. Zhou, J. Y. Xie, *Sol. Stat. Ionics*, **179**,1736 (2008)
8. Z. H. Chen, J.R. Dahn, *J. Electrochem. Soc.*, **149**, 1184 (2002).
9. F. Crose, A. D. Epifanio, J. Hassoun, A. et al., *Electrochem. Sol. Stat. Lett.,* 5, A47 (2002) .
10. S. Tajimi, Y. Ikeda, K. Uematsu, *Sol. Stat. Ionics*, **175**, 287 (2004).
11. S. Franger, F. Le Cras, C. Bourbon, H. Rouault, *J. Power Source.,* **119**, 252(2003)
12. B. Ellis, H. Wang, W. Makahnouk, L. F. Nazar, *J. Mater. Chem.,* **17**, 3248(2007).
13. S. Y. Chung, J. T. Bloking, Y. M. Chiang, *Nature Mate*，**1**, 123 (2002)
14. G. Li, H. Azuma, M. Tohda. *J. Electrochem. Soc*., **149**, 743 (2002).
15. J. Xu, G. Chen, X. Li, *Mater. Chem. Phys.,* **118**, 9 (2009)
16. N. Kalaiselvi, A. Manthiram. *J. Power Sources*, **195**, 2894 (2010)
17. S. F. Yang, Y. P. Zavalij, M. S. Whittingham., *Electrochem. Commun*., **3**, 505 (2001)
18. J. J. Chen, M. S. Whittingham. *Electrochem. Commun.*, 8: 855(2006)
19. K. Kanamura, S. Koizumi, K. Dokko, *J. Mater. Sci.*, **43**, 2138 (2008)
20. Y. X. Zhou, H. B. Yao, Q. Zhang, et al., *Inorgan. Chem.*, **48**, 1082(2009)
21. U. Hiroaki, I. Hiroaki., *Cryst. Grow Des*., **10**, 1777 (2010)
22. Y. Z. Dong, Y M Zhao, H. Duan, *J. Sol. Stat. Electrochem,* **14**, 131 (2010)
23. T. H. Cho, H. T. Chung, *J. Power Sources*, **14**, 1131 (2004).